Konya Mühendislik Bilimleri Dergisi, c. 12, s. 4, 886-907, 2024
Konya Journal of Engineering Sciences, v. 12, n. 4, 886-907, 2024
ISSN: 2667-8055 (Electronic)
DOI: 10.36306/konjes.1461129

OPTIMIZING WASTE HEAT RECOVERY FROM SOLAR COAL GASIFICATION: A COMPARATIVE STUDY OF ORC SYSTEMS USING VARIOUS REFRIGERANTS

[1] Tansel KOYUN, [2,*] Ahmet ELBİR, [3] İbrahim ÜÇGÜL

[1] Suleyman Demirel University, Mechanical Engineering Department, Isparta, TÜRKİYE
[2] Research and Application Center for Renewable Energy Resources, Isparta, TÜRKİYE
[3] Suleyman Demirel University, Textile Engineering Department, Isparta, TÜRKİYE
[1] tanselkoyun@sdu.edu.tr, [2] ahmetelbir@sdu.edu.tr, [3] ibrahimucgul@sdu.edu.tr

Highlights

- R123 exhibits highest energy efficiency (13.93%) and exergy efficiency (11.14%).
- Maximum net power output (261.3 kW) achieved with R123 fluid in ORC system.
- R227ea fluid shows highest total exergy loss (143.71 kW) and mass flow rate (13.11 kg/s).
- Optimal exergy efficiency observed for R113 and R123 in pump, R227ea in condenser, and R365mfa in turbine.

***Corresponding Author:** Ahmet ELBİR, ahmetelbir@sdu.edu.tr

Konya Mühendislik Bilimleri Dergisi, c. 12, s. 4, 886-907, 2024
Konya Journal of Engineering Sciences, v. 12, n. 4, 886-907, 2024
ISSN: 2667-8055 (Electronic)
DOI: 10.36306/konjes.1461129

OPTIMIZING WASTE HEAT RECOVERY FROM SOLAR COAL GASIFICATION: A COMPARATIVE STUDY OF ORC SYSTEMS USING VARIOUS REFRIGERANTS

[1] Tansel KOYUN, [2,*] Ahmet ELBİR, [3] İbrahim ÜÇGÜL

[1] Suleyman Demirel University, Mechanical Engineering Department, Isparta, TÜRKİYE
[2] Research and Application Center for Renewable Energy Resources, Isparta, TÜRKİYE
[3] Suleyman Demirel University, Textile Engineering Department, Isparta, TÜRKİYE
[1] tanselkoyun@sdu.edu.tr, [2] ahmetelbir@sdu.edu.tr, [3] ibrahimucgul@sdu.edu.tr

(Received: 29.03.2024; Accepted in Revised Form: 07.10.2024)

ABSTRACT: In this study, it is aimed to recover the waste heat released as a result of coal gasification and gasification with a solar reactor heat source, with an ORC integrated into the reactor. Thermodynamic analyzes for the integrated system were carried out for a solar reactor (black body solar cavity—receiver) exposed to an average solar flux concentration of 2000 and operating at 1350 K. Assumptions are given for the calculations made in both the gasification reactor and the ORC, and the results are presented in tables and graphs. In the reactor and ORC integrated design, the operation of the integrated ORC sub-cycle with high critical temperature refrigerants (R600, R113, R227ea, R365mfa, R600a, and R123) to recover the heat lost by the $\dot{Q}$uencher (evaporator) in the reactor was investigated. In this designed system, the thermodynamic analysis of the selected refrigerants for ORC was made with the EES software (Engineering Equation Solver). In the ORC system, the best energy and exergy efficiency were obtained for R123 fluid (13.93% and 11.14%), respectively.

Keywords: *Coal Gasification, Refrigerants, Energy Efficiency, Exergy Efficiency, Renewable Energy*

1. INTRODUCTION

Coal gasification is the process of converting coal into a gaseous state by undergoing a series of chemical reactions under high temperature and pressure. Thus, it has been aimed at ensuring that coal is used in a more efficient, clean, and environmentally friendly way and to produce combustible gases with a high calorific value. There are various methods for gasifying coal. Gasification processes taking place in reactors are actually processes that convert carbon monoxide (CO), hydrogen (H_2), and methane (CH_4) from sources such as coal, biomass/waste, and natural gas into an artificial gas, called syngas [1]. The composition and amount of gases produced by the gasification of coals depend on the type and activity of the coal, the type of gases used, and the gasification process applied (pressure, temperature, etc.) [2]. The use of solar energy as a renewable energy source instead of using coal to meet the process heat requirement in the gasification of coal with water vapor has come to the fore as a sustainable and economical practice. Solar reactor coal gasification is a technology used to gasify coal using solar energy. This technology also uses a reactor exposed to intense sunlight and, while heating the coal, also initiates a chemical reaction with gases such as water vapor or carbon dioxide. As a result of this reaction, coal gas is obtained with the transition of the coal to the gas phase and then cooling. Coal gas is a gas mixture containing hydrogen, carbon monoxide, methane, and small amounts of carbon dioxide. This gas mixture can be used both for power generation and for the production of synthetic fuels, chemicals, and other industrial products. Solar reactor coal gasification is considered a more environmentally friendly option over traditional coal burning methods, because it uses solar energy, a clean energy source. This technology may be more efficient than other methods used in coal gas production and produce fewer greenhouse gas emissions. However, solar reactor coal gasification cannot yet be implemented on a commercial scale as it faces some technological and financial hurdles. Investment costs, efficiency of solar energy use, and scale of solar energy collection systems are important in solar reactor design. In addition, environmental impacts such as greenhouse gases produced during the coal gasification process need to be considered.

***Corresponding Author:** Ahmet ELBİR, ahmetelbir@sdu.edu.tr

The Organic Rankine Cycle (ORC) is an energy conversion technology used to convert thermal energy obtained from temperature differences into electrical energy. This cycle is particularly used to convert thermal energy from low temperatures (for example, from geothermal sources or industrial waste temperatures) into electrical energy. The (ORC) works by using an organic fluid. The organic fluid heated by the hot source evaporates, and the resulting steam is converted into electrical energy by passing through the turbine. Then, the steam cooled by the cold source turns back to liquid, and the cycle starts again.

The purpose of coal gasification is to use a higher-energy gas as a fuel than the energy obtained from direct combustion of coal. The purpose of the ORC design is to add to the system as an integrated system that produces energy in order to add sustainability to the high-energy waste heat given to the environment. Waste heat generated during the coal gasification process can be recovered with a thermal power generation technology such as the (ORC). This process increases energy efficiency and ensures environmentally friendly energy production. Many studies have been done on this subject, and some examples are given below: Pierobon, et al. reported twice the thermal efficiency achieved by the (ORC) plants and about the same efficiency as the combined gasification, solid oxide fuel cells, and micro gas turbine plant [3]. In terms of waste heat recovery, Ogorure et al. used the thermal energy from the steam at 290°C obtained from the syngas cooling process for power generation in the ORC and as an energy source for the PEME (Proton Exchange Membrane Electrolyzer). For maximum power generation of the ORC system, R1243zf, R1234yf, R1233zd(E), R1234ze(Z), isobutane, and propane fluids were used. They said that R1233zd(E) is the most suitable working fluid for the ORC configuration [4]. Chen et al. have designed a new integrated supercritical water gasification of the coal system. They showed that the energy and exergy efficiencies of integrated supercritical water gasification of coal systems combined with (ORC)s are higher than those of integrated gasification combined cycles and environmental emissions of integrated supercritical water [5]. In this study, Seyitoglu et al. investigated an integrated coal-based gasification system developed for hydrogen production and electricity generation. In the system studied, an air separation unit, a gasification unit, a gas cooling and cleaning unit, a pressure swing absorption (PSA) unit for hydrogen production, a high temperature electrolyzer for hydrogen production, a Brayton cycle, a steam Rankine cycle, and an (ORC) system were formed [6]. Méndez-Cruz et al. have done a thermodynamic refinement of using a refrigerant as a working fluid in the (ORC). They have worked with R245fa, R600a, R134a and R123 refrigerants. At condensing temperatures above 45 °C, R600a is said to be the most suitable exergetic refrigerant [7]. Kılıç and Arabacı, the performance of the (ORC) was investigated using refrigerants such as R123, R125, R227, R365mfc, and SES36. The researchers noted that the efficiency of the ORC is influenced by the vapor generator temperature, condenser temperature, subcooling temperature, and superheating temperature [8]. Khatoon et al. analyzed the performance of a combined power and cooling system consisting of ORC and VCC (Vapor Compression Cooling). In the VCC system, using refrigerants R123, R134a, and R245fa, they found COP (Coefficient of Performance) values of 2.85, 2.58, and 2.7089, respectively. For the ORC, they utilized Propane and R245fa. By combining R123 in the cooling cycle with propane for the highest temperature value (40°C), they achieved the highest efficiency of 16.48% [9]. Chowdhury et al. They examined the performance of Supercritical CO_2 Brayton cycle (s-CO_2), Triple Cycle (TLC), and (ORC) under constant heat input conditions. They demonstrated that compared to thermal efficiency with s-CO_2 and TLC, a 26.5% higher thermal efficiency can be achieved with n-pentane as the working fluid in the ORC cycle [10]. Jeong and Kang evaluated different refrigerants (R123, R134a, and R245ca) in the cycle they designed. They indicated that R123 refrigerant yielded the highest cycle efficiency. They mentioned that the primary cycle efficiency would be low due to the high temperature at the turbine outlet. For the purpose of recovering heat at the turbine outlet, they stated that in the R245ca cycle, the total COP increased by 47%. In the primary cycle, COP mostly varied with boiler pressure, while in the cycle designed with a recuperator, cycle efficiency varied with boiler temperature [11]. Sun et al. A new waste heat recovery system was proposed to increase energy efficiency and reduce energy consumption in the Rectisol process. This system includes a compression-absorption cascade refrigeration system (CACRS), (ORC) and heat exchanger network (HEN). Using a multi-objective

optimization model, the total annual cost and exergy destruction were minimized. The results showed that waste heat recovery increased by 19.2%, cooling water consumption decreased by 100% and low-temperature cold usage requirement decreased by 1.7%. In the optimal design, the annual cost was determined as $11,082,365 and the exergy destruction was determined as 80,452 kW [12]. Rad et al. A new cogeneration power and cooling load cycle (CPCC) has been developed that targets the efficient and maximum use of waste heat from industrial processes and fossil fuel power plants. This process includes three levels of waste heat recovery, (ORC) and an injection-based cooling process. Thermodynamic performance, cost effectiveness and environmental considerations were examined extensively. With a two-purpose optimization, it was aimed to minimize the total cost and maximize the exergy efficiency. The results showed that CPCC increased exergy performance by 10.3%, reduced exergy destruction by 7.4% and total annual cost by 21.6% compared to the reference system. Additionally, it was found that approximately 11,640 tons of carbon dioxide emissions could be reduced by the injection cooling process [13]. Tera et al. A new polygeneration system integrating biomass gasification, solid oxide fuel cell, gas turbine, (ORC) and supercritical CO_2 Brayton cycle is proposed. The system was simulated in Aspen Plus and energy, exergy, economic and emergy analyzes were performed. Energy and exergy efficiencies were determined as 76.82% and 60.64%, respectively. The adjusted cost of hydrogen is 4.06 $/kg, which is comparable to values in the literature. Annual revenue from sales of hydrogen, heat and electricity can reach $58.42 M. Emergy analysis showed that the system was dependent on purchased inputs but was able to use available resources efficiently. This hybrid system can serve as a low-cost, low-carbon and profitable polygeneration system with low environmental impact in the long term [14]. Braimakis is investigating the potential for electricity savings through waste heat recovery (WHR) from CO_2 compression intercoolers with (ORC) technology. CO_2 discharge pressures from 50 to 500 bar and 3 to 8 compression stages were investigated. While theoretical electricity savings range from 10% to 24%, the maximum savings rate with optimized air-cooled ORCs is approximately 5%. The installed power of WHR-ORC is between 3 and 23 kWe per kg/h of compressed CO_2. Due to changes in the specific heat capacity of CO_2, the waste heat potential depends on the discharge pressure and number of stages. Technical-economic analyzes show payback periods of 6-12 years for 4000 working hours and 2.5-4 years for 8000 hours [15]. Choudhary et al. proposes to use the (ORC) to recover the flue gas waste heat of power plants to reduce energy waste. R245fa working fluid and high ash content Indian coal were used for waste heat recovery from the Integrated Gasification Combined Cycle (IGCC) power plant. As a result of modeling and simulations made with "Cycle-Tempo" software, the energy and exergy efficiencies of the 400 MWe IGCC power plant were found to be 45.50% and 41.62%, respectively, and in the IGCC-ORC integrated system, these efficiencies were determined as 45.84% and 41.92%. ORC produced an additional 2.34 MWe net power, and this additional power production has energy efficiencies of 12.48% and exergy efficiencies of 42.54%. This additional power generation helps avoid approximately 51 tons of CO_2 emissions per day, compared to a similar amount of power produced from coal-based thermal power plants [16]. Aryanfar et al. Three functional modes of a newly designed geothermal power plant were investigated, simulated and analyzed. The first mode is the single flash geothermal cycle (SFGC). The second mode is SFGC with two-stage ORC recovery and the third mode is SFGC with two-stage ORC recovery and LNG cryogenic energy. The addition of a two-stage ORC recovery and LNG cooling exergy cycle aims to increase the thermal and exergy efficiencies of the base SFGC system and utilize the cold energy of LNG before it enters urban consumption networks. ORC's working fluids for the two-stage recovery cycle include R227ea/R116 and R124/R125. The equations of the first and second laws of thermodynamics were used to analyze the proposed system. Assuming two-stage ORC and LNG recovery mode, the energy efficiency of SFGC will increase from 20.23% to 38.63% when using R227ea and R116 working fluids, and from 40.16% to 40.66% when using R124 and R125 working fluids [17]. Li et al. In order to efficiently use waste heat and reduce environmental impacts, a two-absorption organic Rankine cycle (AORC) system was designed and analyzed. To overcome the limitations experienced by traditional ORC systems in effectively utilizing waste heat sources, AORC systems based on absorption heat exchangers have been proposed. The study includes energy, exergy and economic analyzes of three ORC

system models at heat source temperatures between 363.15 K and 413.15 K. The results showed that the AORC system was an optimal waste heat recovery system, able to reduce the outlet temperature to 298.70 K and achieved a high temperature efficiency of 1.037%. The AORC system enabled efficient use of heat resources by facilitating heat exchange with significant temperature differences. In the study, the AORC system exhibited high net power of up to 151.8 kW and electrical exergy efficiency of 55.45%. Moreover, AORC economically outperformed other systems and was found to have the lowest electricity generation cost at heat source temperatures lower than 398.15 K [18]. Yan et al. The effect of waste heat recovery from boiler flue gas on increasing energy use efficiency was examined. Taking a heating station project as an example, the underutilized flue gas waste heat and low energy efficiency of the existing heating system were analyzed. A cogeneration waste heat utilization method with a steam boiler using the (ORC) is proposed. A thermodynamic model was created in MATLAB and the effects of evaporation and condensation temperatures on the waste heat cycle power system were analyzed. Then, the improved cogeneration system was created by using the ORC model in TRNSYS, and the rationality of the remaining heat usage methods was determined by calculation in terms of thermal performance, economy and environmental protection. Simulation results show that the system can produce approximately 552,000 kWh of electricity per year and increase the energy utilization rate from 72% to 78% [19]. Ja'fari et al. The potential of (ORC) to increase energy efficiency and reduce carbon emissions in energy-intensive industries is discussed. The iron and steel industry represents approximately 5% of world energy consumption and a significant amount of waste heat is produced and lost in this sector. Better use of excess waste heat in processes saves energy and increases energy efficiency by increasing the industry's own electricity production. This could ease the burden on energy grids by reducing the increase in electricity consumption brought about by industrial electrification. Additionally, waste heat recovery can significantly reduce carbon emissions and plays an important role in combating global warming. ORC technologies are one of the most suitable technologies for waste heat recovery in the iron and steel industry. This article aims to support the market penetration of these technologies by providing information on ORC design criteria, achievable performance and component costs for waste heat recovery in the iron and steel industry [20]. Mahmoud et al. Ground-cooled (ORC) was studied for waste heat recovery from diesel generator. As a result of simulations made with ANSYS Mechanical APDL, the ground thermal effect radius was calculated as 0.32 m and the ground cycle length was calculated as 1480 m. While ORC with an operating temperature of 300 °C increased the power of the diesel generator by 7.98%, ORC with regeneration increased this increase to 15.31%. The capital costs for the basic ORC are £11,945–18,770 and the payback period is 4.9–7.8 years, while the capital costs for the replacement ORC are £17,062–25,592 and the payback period is 3.7–5.5 years [21]. Cui et al. A new energy allocation strategy is proposed for a solar integrated compressed air energy storage (CAES) system. CAES-based systems with three different energy recovery strategies are compared. CAES–SCS–HP offers 38.9% system power efficiency (SPE) and 99.6% system energy efficiency (SENE). CAES-SCS, on the other hand, shows 57.4% power-to-power (P2P) efficiency with the best cost of energy storage (LCOS) of 0.520 $/kWh. Parametric studies and energy, exergy, economic (3E) analyzes were carried out. While HP integration increases the economic and electrical conversion performance in the low pressure region, ORC integration increases the overall costs of the system but has little effect on exergy loss. The superiority of the proposed CAES and SCS integration strategy has been verified by comparing with existing studies [22].

The novelty of this study is that it offers a systematic approach to increase energy efficiency by using the waste heat generated during the coal gasification process, especially in an integrated manner with solar energy. Compared to existing studies in the literature, this research aims to develop an optimized system in terms of both energy and exergy efficiency by thoroughly examining the performances of different refrigerants (R600, R113, R227ea, R365mfa, R600a and R123) in the (ORC). Additionally, this study shows that integrating the waste heat obtained in the coal gasification process with existing energy conversion technologies is an important step in sustainable energy production. The findings aim to provide a critical basis for future energy systems design, providing more efficient solutions both environmentally and economically.

2. MATERIAL AND METHODS

2.1. Energy and Exergy Analysis for Processes

Efficiency assessment of processes relies significantly on the thorough examination of energy and exergy. The subsequent equations [23] outline the essential formulations for conducting energy and exergy analyzes within a system. At the core of thermodynamic scrutiny lies the foundational mass balance equation, which can be expressed in the steady-state condition as illustrated in Equation (1):

$$\sum \dot{m}_{in} = \sum \dot{m}_{ex} \tag{1}$$

Expressing the mass flow rate as $\dot{m}$ and denoting the states at the outlet and inlet as 'ex' and 'in' respectively, the energy balance can be presented as follows (2):

$$\dot{Q}_{in} + \dot{W}_{in} + \sum_{in} \dot{m} \left(h + \frac{V^2}{2} + gz \right) = \dot{Q}_{ex} + \dot{W}_{ex} + \sum_{ex} \dot{m} \left(h + \frac{V^2}{2} + gz \right) \tag{2}$$

where $\dot{Q}$ is heat transfer rate, $\dot{W}$ is power, h is specific enthalpy, v is velocity,z is elevation and g is gravitational acceleration. The entropy balance equation for steady-state conditions is written in equation (3),

$$\sum_{in} \dot{m}_{in} s_{in} + \sum_{k} \frac{\dot{Q}}{T_k} + \dot{S}_{gen} = \sum_{ex} \dot{m}_{ex} s_{ex} \tag{3}$$

where s is specific entropy, and $\dot{S}_{gen}$ is the entropy generation rate. The exergy balance equation can be written in equation (4),

$$\sum \dot{m}_{in}\, ex_{in} + \sum \dot{E}\, x_{Q,in} + \sum \dot{E} x_{W,in} = \sum \dot{m}_{ex} ex_{ex} + \sum \dot{E} x_{Q,ex} + \sum \dot{E} x_{W,ex} + \dot{E} x_D \tag{4}$$

where $\dot{E} x_D$ is the exergy destruction rate, and can be defined as follows in equation (5),

$$\dot{E} x_D = T_0 \dot{S}_{gen} \tag{5}$$

$\dot{E} x_W$ is the exergy rates releated with work, and is given in equation (6),

$$\dot{E} x_W = \dot{W} \tag{6}$$

$\dot{E} x_Q$ is the exergy rates releated with heat transfer, and is given in equation (7),

$$\dot{E} x_Q = \left(1 - \frac{T_o}{T} \right) \dot{Q} \tag{7}$$

Equation (8) expresses the specific flow exergy:

$$ex = ex_{ph} + ex_{ch} + ex_{pt} + ex_{kn} \tag{8}$$

The kinetic and potential parts of exergy appear in the above equation are assumed to be negligible. Also, chemical exergy is assumed to be negligible [24]. The physical or flow exergy (ex_{ph}) is defined in equation (9),

$$ex_{ph} = (h - h_o) - T_o (s - s_o) \tag{9}$$

where h and s are the specific enthalpy and entropy at the real case, respectively, also, h_o and s_o are

the enthalpy and entropy at the reference environment states, respectively.

The energy efficiency (η) of a system can be defined as equation (10),

$$\eta = \frac{\sum useful\ output\ energy}{\sum input\ energy} \quad (10)$$

The exergy efficiency (ψ) is defined as in equation (11),

$$\psi = \frac{\sum useful\ output\ exergy}{\sum input\ exergy} \quad (11)$$

2.2. Energy and exergy analysis for coal gasification

Coal (T_1, Coal) in Figure 1: As shown in the diagram, coal enters the left reactor (solar reactor) from the upper left corner. Coal is fed into the reactor for gasification. Solar Reactor: This component starts the gasification process by heating coal to high temperatures using solar energy. Solar energy is used to provide thermal energy efficiently. Coal Gasification Reactor: Coal heated in the solar reactor enters this reactor, where it reacts with water vapor (steam) and produces synthesis gas ($CO+H_2$). This process involves a chemical transformation in which coal turns into carbon monoxide (CO) and hydrogen (H_2) gases. Steam (T_2, Vapor): Steam enters the gasification reactor as T_2 and reacts with coal. Steam enables the gasification of coal and plays an important role in the production of synthesis gas. Synthesis Gas (T_1, T_3, T_4, Synthesis Gas $CO+H_2$): Synthesis gas leaving the gasification reactor goes through various stages: T_1, $CO+H_2$: First synthesis gas flow. T_3, $CO+H_2$: Synthesis gas flow before the heat exchanger (HE I. Heat Exchanger). T_4, $CO+H_2$: Post-quencher syngas flow. Heat Exchanger (HE I. Heat Exchanger): Synthesis gas exchanges heat with water here and its temperature is controlled. This step increases efficiency by bringing the temperature of the gas to the desired level. Quencher: It is a component that rapidly lowers the temperature of the synthesis gas. This is important to control the gas and increase its efficiency. This process represents a chemical conversion cycle that involves the production of synthesis gas from coal and the optimization of this gas through various processes. The use of solar energy to increase energy efficiency and reduce carbon emissions are the main advantages of this system.

In Figure 1, the cycle of the coal gasification reactor is shown schematically. According to Figure 1, coal enters the solar reactor at temperature T_1. Only the steam is sent to the reactor by preheating from T_1 to T_2 in the heat exchanger (HE I). The coal and steam reactants entering the solar reactor are heated up to the Treactor temperature. It is assumed that chemical equilibrium will occur in the Treactor. The net energy absorbed in the solar reactor is given as the enthalpy change of the reaction per unit time. Here $\bar{n}$; is the mass flow rate of coal in molar (1 mol s-1)[25]. Quencher (Evaporator) Heat Exchanger" is a type of heat exchanger utilized in industrial cooling systems. In these systems, a fluid (typically water or a refrigerant fluid) flows through a series of tubes or plates, which are metallic structures. The hot gas or liquid in the system is cooled or vaporized through these metallic structures. The term "Quencher" signifies the use of such an evaporator to rapidly cool or vaporize gas or liquid. This is often done to achieve desired temperature, pressure, or other properties of the process fluid. These types of heat exchangers find applications in industrial cooling, air conditioning systems, chemical processes, and many other applications.

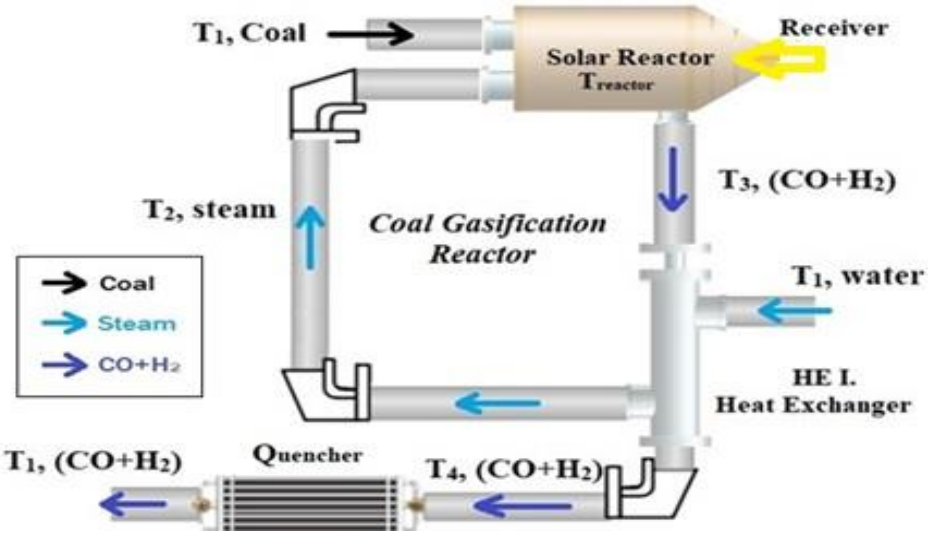

Figure 1. Gasification reactor operating system

In this study, the mole percentages of C, H, and O for the solid fuel (coal) selected were taken as 0.41, 0.40, and 0.19, respectively [26]. Accordingly, equation (12) shows the basic reaction of the gasification of coal with water vapor.

$$CHxOy+(1-y)H_2O = ((x/2)+1-y)H_2 +CO \quad (12)$$

According to equation (12), x and y components are, respectively, *x=H/C=0.40/0.41=0.9756 y=O/C=0.19/0.41=0.4634*

was calculated as follows: According to the data in Table 3, the reaction no. (13) was formed by taking the coal inlet temperature into the solar reactor at 300 K, the water vapor temperature entering the reactor at 1250 K, and the solar reactor temperature at 1350 K.

$$CH0.9756O0.4634(T_1=300K)+0.5366H_2O(T_2=1250K)=1.0244H_2+CO(Treactor=1350K) \quad (13)$$

Moisture content is not taken into account in the reaction equation (13). This reaction is an endothermic one that takes place between 800-1500 K [26].

According to equation (14), the coal temperature T_1 is 300 K, and the x and y stoichiometric coefficients calculated above are substituted to get the reaction equation (15).

$$[C(gr)+(x/2)H_2+(y/2)O_2]+[1+(x/4)-(y/2)]O_2=(x/2)H_2O(g)+CO_2 \quad (14)$$

$$x = H/C \qquad y = O/C$$

$$x = 0.9756 \qquad y = 0.4634$$

$$C + 0.4878H_2 + 1.2439O_2 = 0.4878H_2O + CO_2 \quad (15)$$

According to the information in Equation (15), the following intermediate equation is used to calculate the formation enthalpy of coal.

$$\bar{H}_i = \bar{H}_i^0 + m\int_{300}^{T_2} \bar{C}_p\, dT = m[\bar{h}_{fi}^0 + (\bar{h}^0 - \bar{h}_{300}^0)] \quad (16)$$

According to this intermediate equation, the molar enthalpies of the components (H_2O, H_2, and CO) at different temperatures were calculated and shown in Table 1. Equation (17) was used to calculate the

formation enthalpy of coal. In this equation, the intermediate equation values calculated for the components (H_2O, H_2, and CO) excluding coal and the formation enthalpy values [12] belonging to these components and taken from the tables are written in equation (17), and the formation enthalpy value for coal is calculated.

$$\bar{H}_f^o = \bar{H}^0_{CH_{0.9756}O_{0.4634}} = 0.4878\bar{H}^0_{H_2O} + \bar{H}^0_{CO_2} - \bar{H}^0_C - 0.4878\bar{H}^0_{H_2} - 1.2439\bar{H}^0_{O_2} \quad (17)$$

The molar enthalpy of formation of coal is calculated as $\bar{H}_f^0 = -511485.21$ kJ/kmol.K

Table 1. The molar enthalpy values of the components according to the basic equation

	$\bar{H}_f^0$ (kJ/kmol)	$\bar{H}_{300}$ (kJ/kmol)	$\bar{H}_{1250}$ (kJ/kmol)	$\bar{H}_{1350}$ (kJ/kmol)
$CH_{0.9756}O_{0.4634}$	-511485.21	-	-	-
H_2O	-241827	9966	46579.5	51066.5
H_2	0	8522	36813.75	39947.75
CO	-110530	8723	38810	42266

The molar entropy values for the coal components are calculated according to the following intermediate equation (18):

$$\bar{S}_i = \bar{S}^0_{fi} + (\bar{S}^0 - \bar{S}^0_{300}) \quad (18)$$

The molar entropies of the components were calculated according to equation (18) and are given in Table 2. In addition, the formation entropy values of the components are taken from the tables to calculate the coal formation entropy [27]. Thus, the molar formation entropy of the coal was calculated by substituting the necessary data according to equation (19).

$$\bar{S}_f^0 = \bar{S}^0_{CH_{0.9756}O_{0.4634}} = 0.4878\bar{S}^0_{H_2O} + \bar{S}^0_{CO_2} - \bar{S}^0_C - 0.4878.\,\bar{S}^0_{H_2} - 1.2439 \quad (19)$$

The result calculated for equation (19) was found as $\bar{S}_f^0 = -18.6102$ kJ/kmol.K

Table 2. Entropy values of the components according to the basic equation

	$\bar{S}_f^0$ (kJ/kmol.K)	$\bar{S}_{300}$ (kJ/kmol.K)	$\bar{S}_{1250}$ (kJ/kmol.K)	$\bar{S}_{1350}$ (kJ/kmol.K)
$CH_{0.9756}O_{0.4634}$	-18.6102	-	-	-
H_2O	188.833	188.928	242.1275	245.579
H_2	130.574	130.754	172.9452	175.3577
CO	197.568	197.723	241.961	244.623

While performing the exergy analysis of the integrated system, the solar reactor in Figure 1 was first discussed. Solar reactor at Treactor temperature, which is the heat source of the coal gasification cycle, is assumed as the cavity receiver. The absorption capacity of solar energy collected in the solar reactor is expressed by the solar energy absorption efficiency (ηabsorpsiyon). Parameter and temperature values of the solar reactor are; T_1=300 K, T_2=1250 K, Treactor=1350 K, T_3=1350 K, T_4=940 K, P=1 bar, I=1kW/m2, C=2000 [23].

Solar energy absorption efficiency is given by equation (20).

$$\eta_{absorption} = \frac{\dot{Q}_{reactor,net}}{\dot{Q}_{solar}} = 1 - \left(\frac{\sigma\, T^4_{reactor}}{IC}\right) \quad (20)$$

Here;

Qreactor-net = Net energy absorbed
Qsun = Solar energy from the solar condensation system to the reactor
I = Direct radiation (the amount of direct radiation from the sun)
C = Average flux concentration (condensation rate) coming onto the solar reactor
Treaktör = Reactor temperature
σ = Stefan–Boltzmann constant (5.67 x 10-8 Wm-2K-4)

$\dot{Q}_{reaktör,net}$ in equation (20) is calculated according to equation (21)

$$\dot{Q}_{reactor,net} = \dot{n}\Delta\bar{H}|_{coal@T_1,H_2O@T_2\rightarrow \text{products}@T_{reactor}} \quad (21)$$

Here ($\dot{n}$) is the mass flow rate of the coal (1 g s-1) [10].

For a continuous flow open system, the heat transfer rate is calculated according to Equation (22) [12].

$$\bar{Q} = \sum \bar{n}_{ex}\left(\bar{h}_f^0 + \bar{h} - \bar{h}^0\right)_{ex} - \sum \bar{n}_{in}\left(\bar{h}_f^0 + \bar{h} - \bar{h}^0\right)_{in} \quad kj/kmol \quad (22)$$

The enthalpy values required in equation (22) were taken from Table 2, and the heat transfer rate $\dot{Q}$ value was calculated as 28.275 kW.

The irreversibility in the solar reactor is calculated according to the equation (23) given below [14].

$$\Delta\dot{S}_{gen} = \frac{\dot{Q}_{solar}}{T_{reactor}} + \frac{\dot{Q}_{radiation\ loss}}{T_1} + \dot{n}\Delta s|_{coal@T_1,H_2O@T_2\rightarrow products@T_{reactor}} + \dot{n}\Delta s_{mix} \quad (23)$$

According to Equation (23) Radiation losses (Qradiation losses) are the losses due to radiation from the reactor at Treactor temperature to the environment at T_1 temperature, calculated according to equation (24)[1].

$$\dot{Q}_{\text{radiation loss}} = \left(1 - \eta_{\text{absorption}}\right)\dot{Q}_{\text{solar}} \quad (24)$$

Δsmix in equation (23) is the mixture entropy resulting from the mixture of gases; it is calculated according to equation (25).

$$\Delta s_{mix} = -\sum R_i y_i \ln x_i \quad (25)$$

In Equation (26) the special gas constant Ri is

$$R_i = R_{mix}\frac{x_i}{y_i} \quad (26)$$

According to Equation 27, the entropy of the mixture is

$$\Delta s_{mix} = -R_{mix}\sum_{i=1}^{N} x_i \ln x_i \quad (27)$$

It is calculated as (0.8227 kJ/kg.K for R_{mix}The results for the solar reactor are; $\dot{Q}_{solar}$=30,76 (kW), $\dot{Q}_{radiationloss}$=2,7684 (kW), $\dot{n}\Delta s$=0,015325 (kW/K), $\dot{n}\Delta S_{mix}$=0,0010943 (kW/K), $\Delta\dot{S}_{gen}$=0,0483 (kW/K).

In the exergy calculation, the Heat Exchanger (HE I) in Figure 1 is considered as the second. Water (H_2O) enters the heat exchanger (HE I) at ambient temperature T_1 and leaves at temperature T_2. The products enter the heat exchanger (HE I.) at T_3 temperature and leave at T_4 temperature. The composition of the reactants and products remains unchanged during the heating and cooling processes in the heat exchanger. Accordingly, the heat transfer rate (Qheat exchange) given from the products to the water was

calculated according to equation (28).

$$\dot{Q}_{heat\ exchanger} = \dot{n}\Delta h|_{H_2O@T_1 \rightarrow H_2O@T_2} = \dot{n}\Delta h|_{products@T_3 \rightarrow products@T_4} \quad (28)$$

Here, the enthalpy values corresponding to T_1 and T_2 temperatures were calculated as 1.019 kW, assuming that water vapor is an ideal gas [23]. Likewise, enthalpy values corresponding to T_3 and T_4 temperatures for ($CO+H_2$) are taken from Table 1 by assuming an ideal gas. Thermodynamic results for the heat exchanger are; $\dot{Q}_{heat\ exchanger}$=1,3 (kW), Irreversibility=0,002555 (kW/K), $\dot{n}\Delta s$=0,0014 (kW/K), $\Delta\dot{S}_{gen}$=0,001155 (kW/K).

The term $\dot{n}\Delta h|_{products@T_3 \rightarrow products@T_4}$ in Equation (28) is the enthalpy values for products ($CO+H_2$) for T_3 = 1350 K and T_1 = 300 K for the case where there is no heat exchanger, assuming ideal gas. It is taken from Table 3, and its value is calculated as 3.21 kW.

Accordingly, the heat exchanger efficiency was calculated as 40% according to equation (29).

$$\eta_{heatexchanger} = \frac{\dot{Q}heatexchanger}{\dot{n}\Delta h|_{products@T_3 \rightarrow products@T_1}} \quad (29)$$

$$\Delta\dot{S}_{gen,\ heatexchanger} = \dot{n}\Delta s|_{H_2O@T_1 \rightarrow H_2O@T_2} + \dot{n}\Delta s|_{products@T_3 \rightarrow products@T_4} \quad (30)$$

In the exergy calculation, exergy analysis was performed for the Quencher (evaporator) in Figure 1 as the third. After the products exit the heat exchanger, they are rapidly cooled to ambient temperature (T_1).

The heat transfer rate transferred during cooling is given by equation (31),

$$\dot{Q}\text{cooling} = \dot{n}\Delta h|_{products@T_4 \rightarrow products@T_1} \quad (31)$$

It is calculated according to equation (31). Here, for T_1=300 K and T_4=940 K, the products ($CO+H_2$) are accepted as ideal gases, and the required enthalpy values are taken from Table 1. Accordingly, $\dot{Q}$cooling is calculated at 1.9025 kW.

The irreversibility equation during cooling is (32).

$$\Delta\dot{S}_{gen} = \frac{\dot{Q}_{quencher}}{T_1} + \Delta s|_{products@T_4 \rightarrow products@T_1} \quad (32)$$

Accordingly, the total irreversibility is calculated as 9.712 W/K according to equation (32).

The heat transfer rates, irreversibility, and thermal efficiencies for the three main components (solar reactor, heat exchanger, and Quencher) in the gasification reactor were calculated by taking the mass flow rate of the coal (1 mol s-1) and the results are given in Table 3.

Table 3. Shows the heat transfer rate and irreversibility values for the three main components in the gasification reaction

Gasification cycle Components	$\dot{Q}_{heat}$ **[kW]**	**Irreversibility [kW/K]**
Solar reactor	28.275	0.0483
Heat exchanger I.	1.3	0,002555
Quencher	1.9025	0.009712

R600 (n-Butane): The chemical formula of the R600 refrigerant is C4H10. Its molecular weight is 58.12 g/mol. Its boiling point is -0.5 °C. Its liquid density is 601 kg/m³. Its ozone depletion potential (ODP) is 0. Its global warming potential (GWP) is 3.

R113 (1,1,2-Trichloro-1,2,2-trifluoroethane): The chemical formula of the R113 refrigerant is C2Cl3F3. Its molecular weight is 187.38 g/mol. Its boiling point is 47.6 °C. Its liquid density is 1560 kg/m³. Its ozone

depletion potential (ODP) is 0.8. Its global warming potential (GWP) is 6130.

R227ea (1,1,1,2,3,3,3-Heptafluoroethane): The chemical formula of the refrigerant R227ea is C3HF7. Its molecular weight is 170.03 g/mol. Its boiling point is -16.4 °C. Its liquid density is 1407 kg/m³. Its ozone depletion potential (ODP) is 0. Its global warming potential (GWP) is 3220.

R365mfa (1,1,1,3,3-Pentafluoro-3-methoxypropane): The chemical formula of the refrigerant R365mfa is C4H5F5O. Its molecular weight is 148.08 g/mol. Its boiling point is 40.2 °C. Its liquid density is 1300 kg/m³. Its ozone depletion potential (ODP) is 0. The global warming potential (GWP) is 804.

R600a (Isobutane): The chemical formula of the refrigerant R600a is C4H10. Its molecular weight is 58.12 g/mol. Its boiling point is -11.7 °C. Its liquid density is 551 kg/m³. Its ozone depletion potential (ODP) is 0. Its global warming potential (GWP) is 3.

R123 (2,2-Dichloro-1,1,1-trifluoroethane): The chemical formula of the refrigerant R123 is C2HCl2F3. Its molecular weight is 152.93 g/mol. Its boiling point is 27.85 °C. Its liquid density is 1460 kg/m³. Its ozone depletion potential (ODP) is 0.02. Its global warming potential (GWP) is 79.

2.3. Energy and exergy analysis for ORC

The extended system description in Figure 2 covers an integrated energy conversion process that includes both coal gasification and the (ORC): Coal Gasification Process: Coal (T_1, Coal): Entry Point: Enters the left reactor from the upper left corner. Function: Basic raw material for the gasification process. Solar Reactor: Entry Point: Coal enters as T_1. Function: Using solar energy, it raises coal to high temperatures and starts the gasification process. Coal Gasification Reactor: Entry Points: Coal and steam heated in the solar reactor enter as T_2. Function: It enables the reaction of coal and steam to produce synthesis gas ($CO+H_2$). Steam (T_2, Vapor): Entry Point: Enters the gasification reactor. Function: It reacts with coal and supports the gasification process. Synthesis Gas (T_1, T_3, T_4, $CO+H_2$): T_1: The first synthesis gas flow exits the gasification reactor. T_3: Synthesis gas flow before heat exchanger (HE I). T_4: Syngas flow after quencher. Heat Exchanger (HE I. Heat Exchanger): Entry and Exit Points: Provides heat exchange between water and synthesis gas. Function: Controls and optimizes the temperature of the gas. (ORC): Quencher: Entry and Exit Points: T_4 ($CO+H_2$) enters and T_5 ($CO+H_2$) exits. Function: Rapidly lowers the temperature of synthesis gas. Pump: Inlet and Outlet Points: It takes the cooled synthesis gas and pressurizes it. Function: Controls gas flow and regulates system pressure. Heat Exchanger (HE II. Heat Exchanger): Inlet and Outlet Points: Refrigerant enters at T_6 and exits at T_9. Function: Provides heat exchange between synthesis gas and refrigerant. Turbine: Entry and Exit Points: At T_5, synthesis gas enters and the turbine rotates and produces energy. Function: Converts the kinetic energy of synthesis gas into mechanical energy and eventually into electrical energy. Refrigerant: Types: Different refrigerants such as R600, R113, R227ea, R365mfa, R600a, R123 are used. Function: It circulates in heat exchangers and ensures efficient transfer of heat. This integrated system combines coal gasification and the (ORC) to efficiently produce both thermal energy and electrical energy. The use of solar energy allows the system to benefit from renewable energy sources and reduces carbon emissions.

The coal gasification process takes place at high temperatures, and waste heat is generated during the process. One of the methods for recovering this waste heat is by integrating ORC into the system. The ORC system uses waste heat to evaporate an organic liquid. The evaporated liquid is converted by a turbine to generate electrical energy. In this way, an additional energy source is obtained by using the waste heat generated during the coal gasification process. Figure 2 shows schematically the recovery of waste heat from coal gasification with ORC.

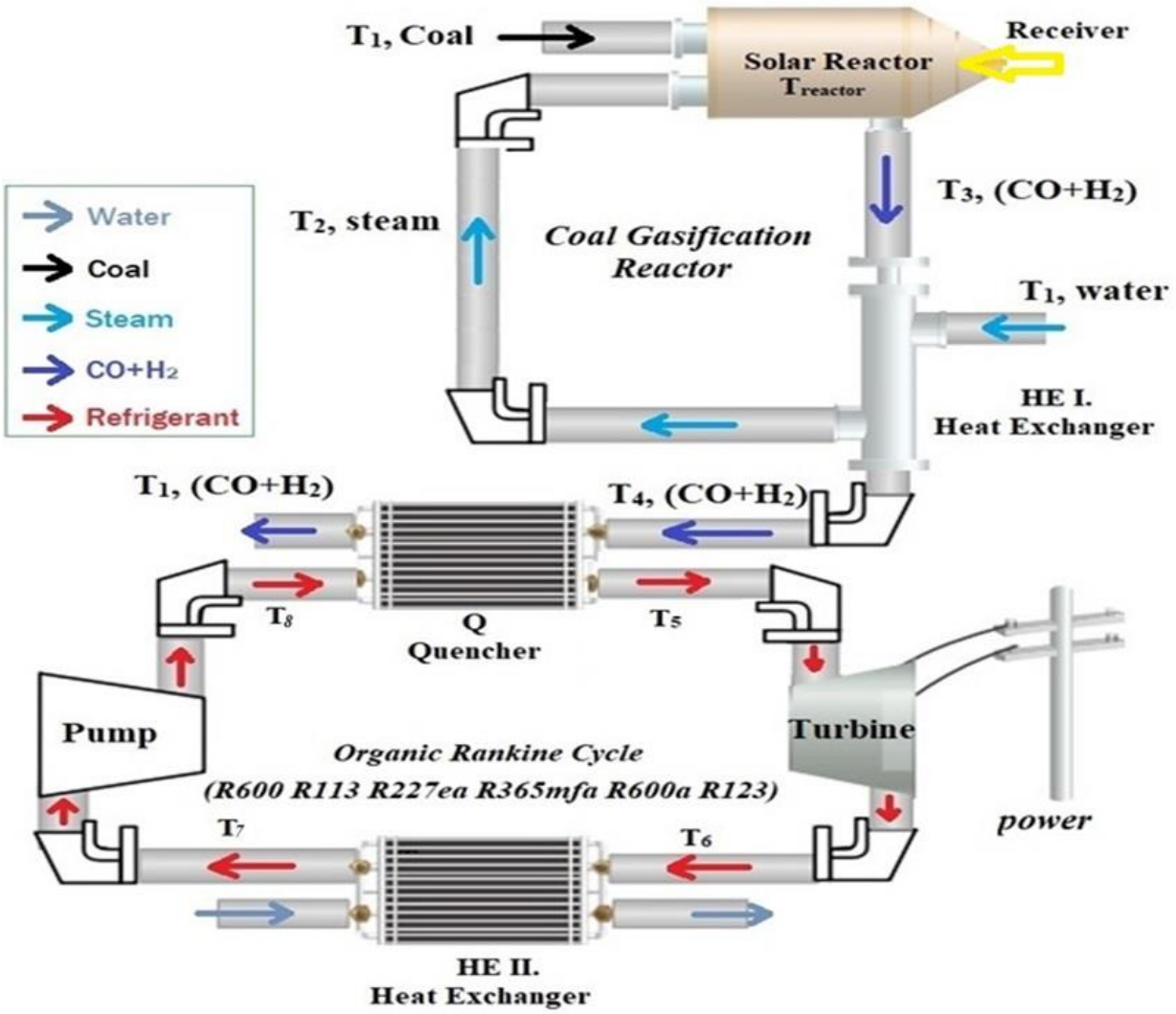

Figure 2. Recovery of the heat released during the solar gasification of coal with an ORC system

For ORC system thermal efficiency (η) in equation (33),

$$\eta_{ORC} = \frac{\dot{W}_{turb.}}{\dot{Q}_{evap.}^{ORC} + \dot{W}_{pump.}} \tag{33}$$

ORC system exergy efficiency (ψ) in equation (34),

$$\psi_{ORC} = \frac{\dot{W}_{turb.}}{Ex_{evap.}^{ORC} + W_{pump.}} \tag{34}$$

The assumptions for ORC in the system designed in the study are given below.

Acceptances

- heat taken from the evaporator and the heat discharged from the condenser were transferred without loss.
- The mass flow rate of the refrigerant in the ORC is kept constant.
- Pressure losses are neglected in all components of the ORC.
- Evaporation Dew point temperature is accepted as 90 ^{0}C, Condenser Dew point temperature is 20 ^{0}C and Dead state (T_0.)temperature is 15 ^{0}C for ORC.
- The variations in kinetic and potential energy are not consideable

- For each fluid, evaporator 90 ^{0}C in ORC, condenser 20 ^{0}C, turbine efficiency 85%, pump efficiency 75% are calculated as constant.
- Waste heat loss transferred from Quncher to ORC was taken as zero.
- ORC thermodynamic analysis was calculated with the EES (Engineering Equation Solver) software [28].
- The flow rate of the fluid used in the gasification reactor (passing through the Quencher) was accepted as 1 g/s. Calculations were made by taking the mass flow rate unit (kg/s) of the fluid used in the ORC system.
- For the gasification reactor analyses in the study, the previous gasification analyses by the authors and included in the literature were taken as a basis [29].

3. RESULTS AND DISCUSSION

The temperature entropy T-s diagrams of the cycles are shown in figure 3(R600), figure 4(R113), figure 5(R227ea), figure 6(R365mfa), figure 7(R600a) and figure 8(R123).

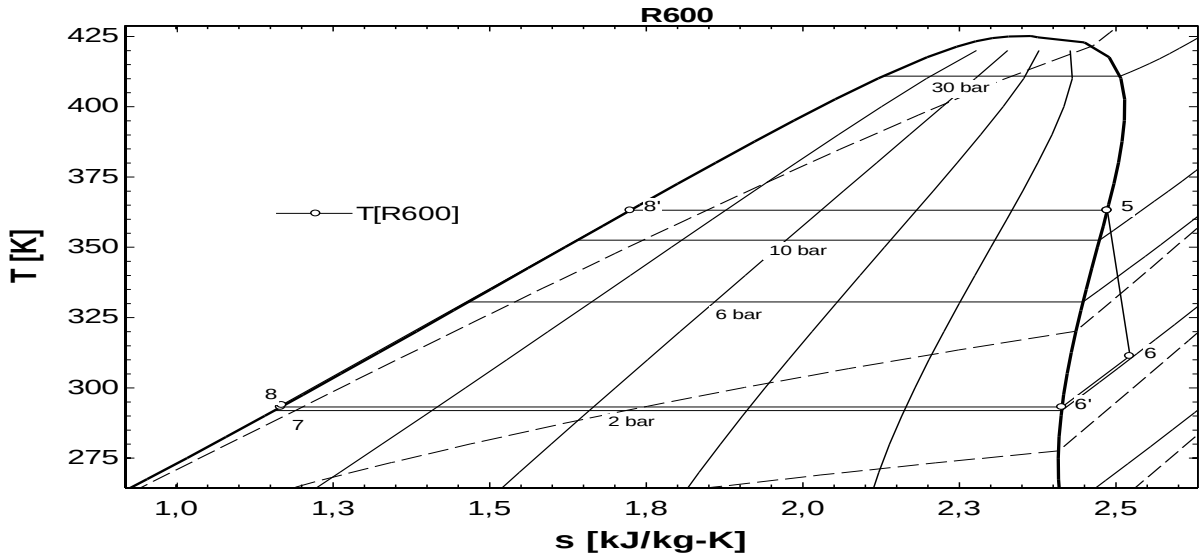

Figure 3. *T-s diagram for R600 ORC*

Table 4. gives the thermodynamic values of the state points of the R600 cycle in the integrated system in Figure 3.

Table 4. Thermodynamic values for R600 ORC

Location	T [K]	s [kJ/kg.K]	P [bar]	h [kJ/kg]	ex []
T_0.	288,2	2,503	1	609,9	
5.	363,2	2,486	12,51	709	103,9
6.	311,4	2,522	2,083	645,9	30,33
6′.	293,2	2,414	2,083	613,1	28,8
7.	293,2	1,167	2,083	247,4	22,57
8.	294	1,169	12,51	249,8	24,38
8′.	363,2	1,725	12,51	432,5	46,81

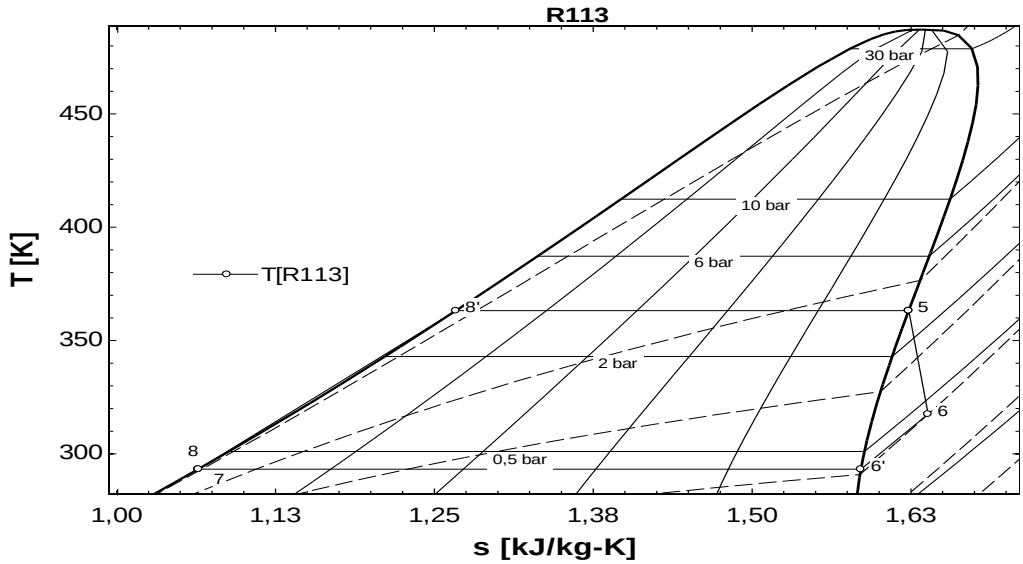

Figure 4. *T-s diagram for R113 ORC*

Table 5 gives the thermodynamic values of the state points of the R113 cycle in the integrated system in Figure 4.

Table 5. Thermodynamic values for R113 ORC

Location	T [K]	s [kJ/kg.K]	P [bar]	h [kJ/kg]	ex []
T_0.	288,2	1,048	1	213,8	-------
5.	363,2	1,623	3,434	414,2	34,73
6.	317,5	1,638	0,3669	387,2	3,334
6′.	293,2	1,586	0,3669	371	2,435
7.	293,2	1,064	0,3669	218,1	-0,1506
8.	293,3	1,064	3,434	218,4	0,04518
8′.	363,2	1,267	3,434	284,8	8,002

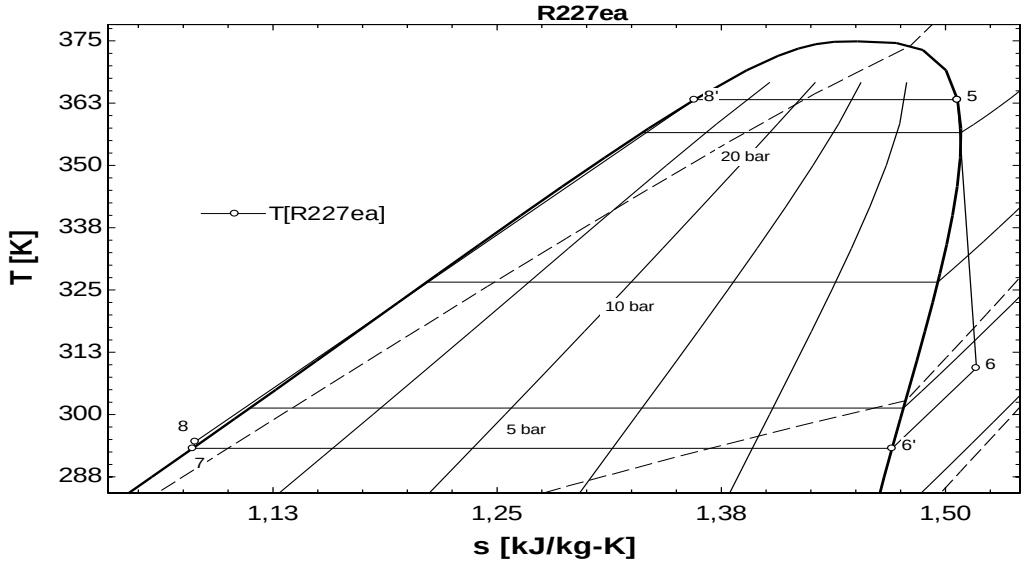

Figure 5. T-s diagram for R227ea ORC

Table 5 gives the thermodynamic values of the state points of the R227ea cycle in the integrated system

in Figure 5.

Table 6. Thermodynamic values for R227ea ORC

Location	T [K]	s [kJ/kg.K]	P [bar]	h [kJ/kg]	ex []
T_0.	288,2	1,536	1	338,3	-------
5.	363,2	1,507	23	369,7	39,91
6.	309,4	1,517	3,896	351,4	18,49
6′.	293,2	1,47	3,896	337,2	17,88
7.	293,2	1,08	3,896	222,9	15,93
8.	294,6	1,082	23	224,7	17,29
8′.	363,2	1,36	23	316,5	28,92

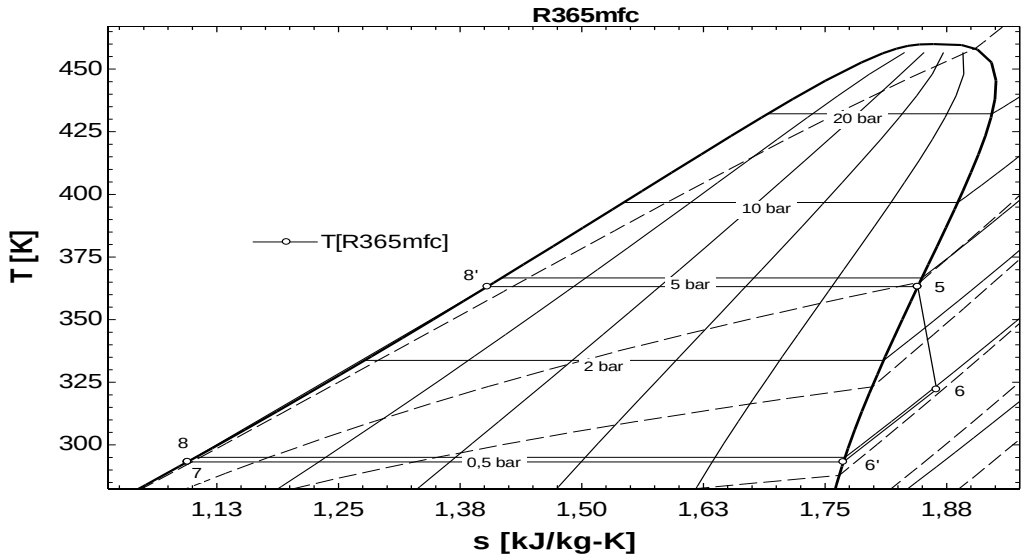

Figure 6. T-s diagram for R365mfc ORC

Table 7 gives the thermodynamic values of the state points of the R365mfc cycle in the integrated system in Figure 6.

Table 7. Thermodynamic values for R365mfc ORC

Location	T [K]	s [kJ/kg.K]	P [bar]	h [kJ/kg]	ex []
T_0.	288,2	1,072	1	220,2	-------
5.	363,2	1,845	4,585	488,8	45,63
6.	322,2	1,865	0,4628	453,9	5,212
6’.	293,2	1,769	0,4628	424,5	3,359
7.	293,2	1,095	0,4628	226,9	-0,01192
8.	293,3	1,095	4,585	227,3	0,3151
8’.	363,2	1,403	4,585	328,2	12,48

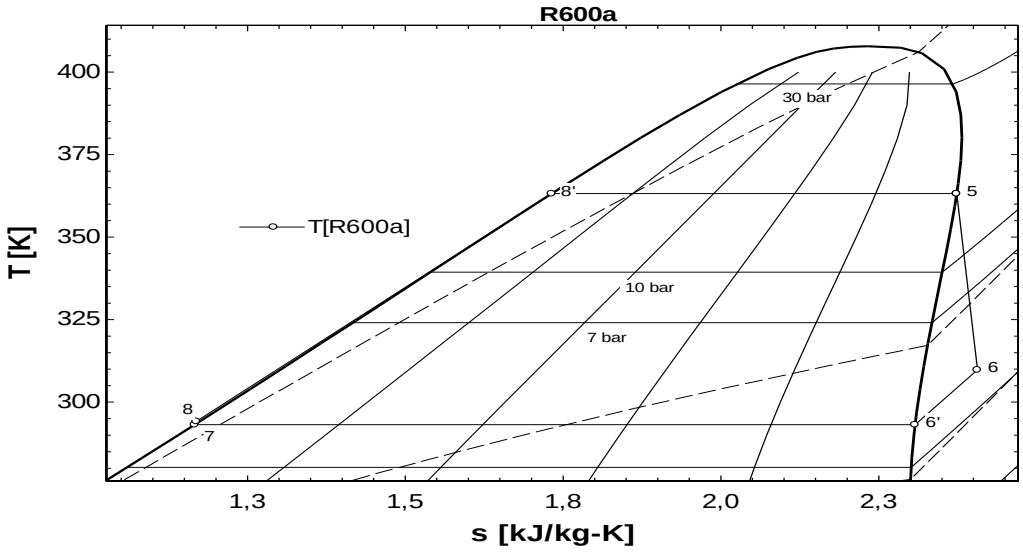

Figure 7. T-s diagram for R600a ORC

Table 8 gives the thermodynamic values of the state points of the R600a cycle in the integrated system in Figure 7.

Table 8. Thermodynamic values for R600a ORC

Location	T [K]	s [kJ/kg.K]	P [bar]	h [kJ/kg]	ex []
T_0.	288,2	2,459	1	582,3	-------
5.	363,2	2,373	16,42	668,6	110,9
6.	309,8	2,406	3,024	611,7	44,47
6′.	293,2	2,307	3,024	581,9	43,16
7.	293,2	1,166	3,024	247,4	37,46
8.	294,2	1,169	16,42	250,6	39,88
8′.	363,2	1,732	16,42	435,6	62,74

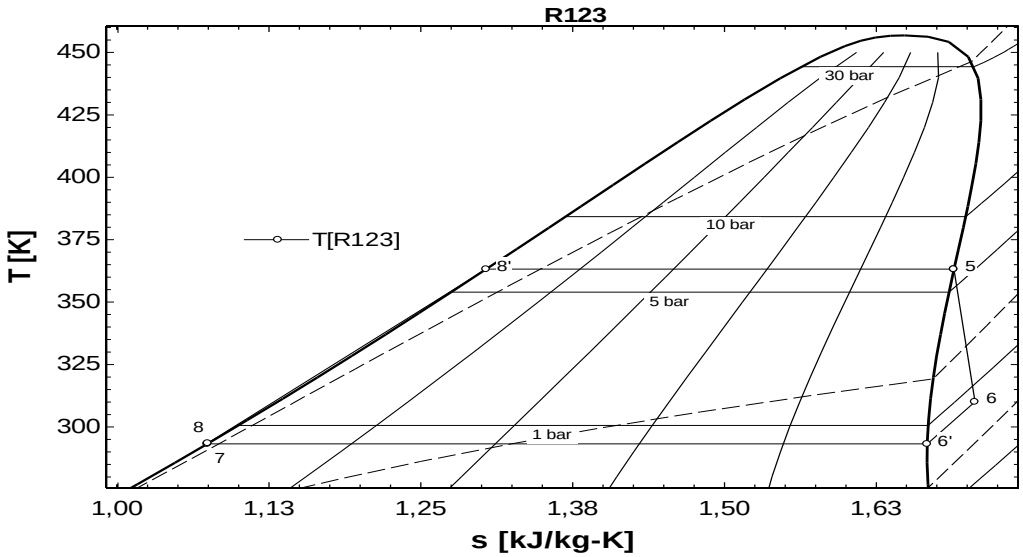

Figure 8. *T-s diagram for R123 ORC*

Table 9 gives the thermodynamic values of the state points of the R123 cycle in the integrated system in Figure 8.

Table 9. Thermodynamic values for R123 ORC

Location	T [K]	s [kJ/kg.K]	P [bar]	h [kJ/kg]	ex []
T_0.	288,2	1,057	1	215,9	-------
5.	450	1,698	32,88	465,8	65,05
6.	319,2	1,727	0,7586	413,4	4,211
6′.	293,2	1,667	0,7586	394,9	3,036
7.	293,2	1,074	0,7586	221,1	0,04336
8.	295	1,077	32,88	224	2,236
8′.	450	1,587	32,88	415,7	47,05

In the ORC system integrated into the solar reactor, R600, R113, R227ea, R365mfa, R600a, R123 refrigerants were tested one by one, and the thermodynamic parameters, especially the energy and exergy efficiencies of the system, are given in Table 10.

Table 10. Thermodynamic results of different fluids in the ORC system

	R600	R113	R227ea	R365mfa	R600a	R123
Energy Efficiency (%η)	13.68	13.78	12.51	13.31	13.52	13.93
Exergy Efficiency (%ψ)	10.92	10.81	10	10.27	10.83	11.14
Condenser (%ψ)	87.59	82.7	85.65	74.11	88.6	88.5
Evaporator (%ψ)	83.87	85.81	75.5	83.94	82.21	86
Pump (%ψ)	75.48	75.43	75.52	75.44	75.5	75.52
Turbine(%ψ)	85.84	86.06	85.81	86.26	85.79	85.82
Mass Flow Rate ($\frac{kg}{s}$)	4.143	9.718	13.11	7.276	4.551	8.835
Net Power (kW)	251.75	260.08	217.46	250.55	244.62	261.3
Condenser $Ex_{D.}$(kW)	3.99	5.858	4.816	9.843	3.637	3.635
Evaporator $Ex_{D.}$(kW)	63.37	55.76	96.24	63.1	69.88	54.98
Pump $Ex_{D.}$(kW)	2.439	0.6197	5.786	0.7748	3.574	1.076
Turbine $Ex_{D.}$(kW)	43.17	42.54	39.87	40.43	42.93	43.88
Turbine $\eta_{isentropic}$	85	85	85	85	85	85
Pump $\eta_{isentropic}$	75	75	75	75	75	75

In Figure 3, the energy and exergy efficiencies for the refrigerants (R600, R113, R227ea, R365mfa, R600a, and R123) used in the ORC system are shown.

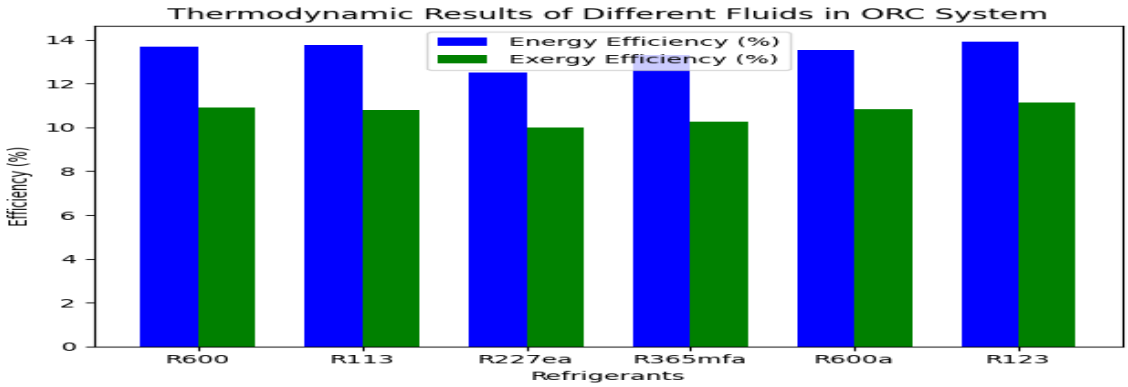

Figure 3. Energy and exergy efficiency of fluids (R600, R113, R227ea, R365mfa, R600a, R123) used in the ORC system

As depicted in Figure 3, among the fluids analyzed for energy and exergy efficiency within the ORC system, R123 exhibited the highest values, with energy efficiency at 13.93% and exergy efficiency at 11.14%. In a related study, it was reported that R123 and Ammonia are the most suitable fluids for ORC, boasting high energy and exergy efficiency throughout the entire cycle [30].

Figure 4 shows exergy efficiency values for different refrigerants (R600, R113, R227ea, R365mfa, R600a, and R123) and components (pump, condenser, evaporator, and turbine) in the ORC system.

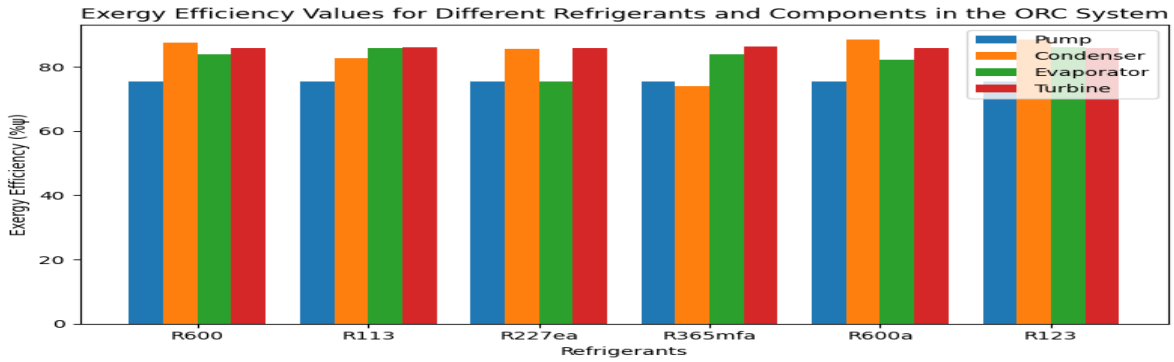

Figure 4. Exergy efficiencies of ORC System components (pump, condenser, evaporator, turbine) according to six different fluids (R600, R113, R227ea, R365mfa, R600a, R123)

As illustrated in Figure 4, the components and refrigerants exhibiting the highest exergy efficiency among ORC system components were determined to be R113 and R123 for the pump, R227ea for the condenser, R123 for the evaporator, and R365mfa for the turbine.

Figure 5 shows the exergy destruction values for different refrigerants (R600, R113, R227ea, R365mfa, R600a, and R123) and components (pump, condenser, evaporator, and turbine) in the ORC system.

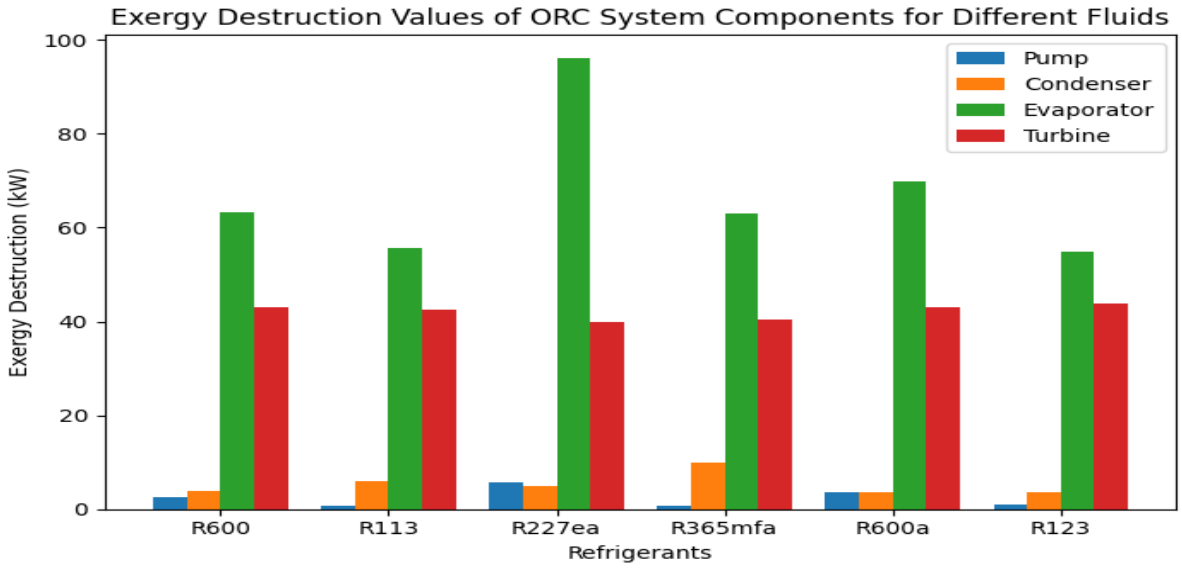

Figure 5. Exergy destruction values of ORC System components (pump, condenser, evaporator, turbine) according to six different fluids (R600, R113, R227ea, R365mfa, R600a, R123)

As depicted in Figure 5, the ORC components with the highest exergy losses were identified as the evaporator, turbine, condenser, and pump, respectively. Among the fluids utilized, R227ea exhibited the highest exergy loss, while R123 refrigerant demonstrated the least exergy loss.

Figure 6 shows the net power, total exergy and mass flow values obtained for each of the six different fluids (R600, R113, R227ea, R365mfa, R600a, R123) used in the ORC system.

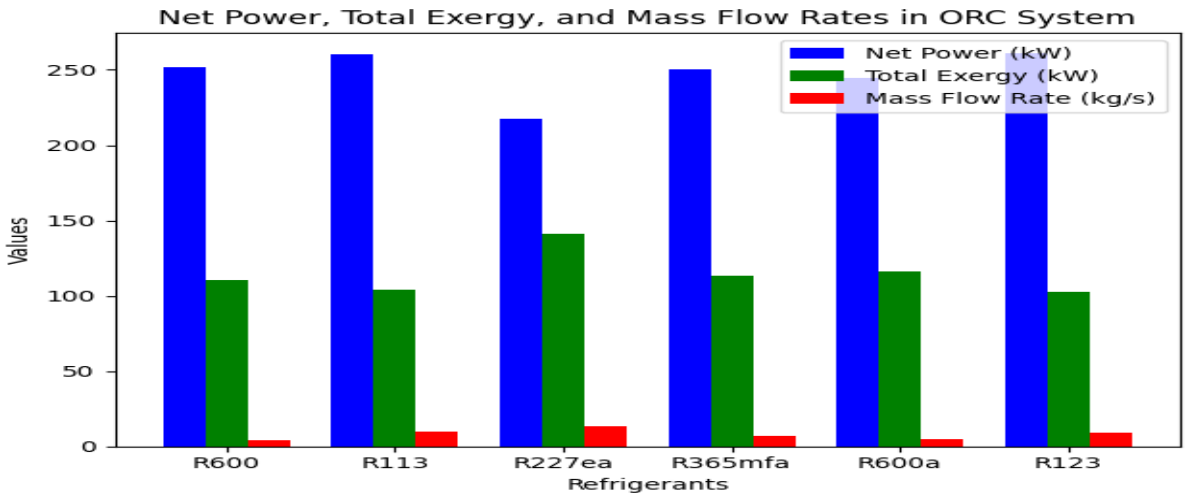

Figure 6. Net power, total exergy and mass flow rates of different fluids (R600, R113, R227ea, R365mfa, R600a, R123) in the ORC system

As illustrated in Figure 6, the calculations revealed that for the R123 fluid, the highest net power output (261.3 kW), the highest total exergy loss (143.71 kW), and the highest mass flow rate (13.11 kg/s) were observed for the R227ea fluid.

In terms of Energy and Exergy Efficiency, R123 fluid has energy efficiency of 13.93% and exergy efficiency of 11.14%. In the literature: Pierobon et al. In his study, higher energy efficiency values were obtained for ORC systems, but specific values were not given. Ogorure et al. Optimal efficiency with R1233zd(E) is stated, but numerical data is missing.

In terms of Refrigerant Performance, high efficiencies have been achieved with R123, R600a and R113. In the literature: Kılıç and Arabacı made similar performance evaluations using fluids such as R123, R125, R227, R365mfc, but did not specify specific efficiencies. Méndez-Cruz stated that R600a is most suitable at temperatures above 45°C.

In terms of Power Output, 261.3 kW net power with R123, 217.46 kW with R227ea. In the literature: Khatoon et al. Using ORC and R245fa, 2.34 MWe net power generation was achieved. This is a larger system than the size of the current study.

In terms of Condenser and Evaporator Efficiency, condenser efficiency with R600a is 88.6%, evaporator efficiency with R113 is 85.81%. In the literature: The performance of R600a is stated to be high, but comparative values are rarely given.

In terms of Flow Rates, 13.11 kg/s for R113, 4.143 kg/s for R600. In the literature: Flow rates are generally not given in detail, so it is difficult to make specific comparisons.

This work is highly competitive with the efficiencies and power output you state relative to many studies in the existing literature. Especially the high energy and exergy efficiency provided by R123 shows that this system offers an effective design. Additionally, detailed analysis of fluids and performance comparisons make this work even more original. In this context, we can say that this study makes a significant contribution to the existing literature in terms of efficiency and power production.

4. CONCLUSION AND SUGGESTIONS

The study investigated the energy and exergy analysis involved in extracting waste heat from solar coal gasification through an integrated ORC system. Various refrigerants were examined within the ORC system to harness electrical energy from the waste heat of a coal gasification system. The findings highlight several key points:

The highest energy efficiency was found in R123 fluid (13.93%), while the lowest was observed with R227ea (12.51%). This indicates that R123 performs better in the system. The highest exergy efficiency was

again observed in R123 fluid (11.14%), while the lowest was observed in R227ea (10.00%). High exergy efficiency indicates that the system works more effectively. The highest capacitor efficiency was seen with R600a (88.6%), and the lowest was recorded as R365mfa (74.11%). Evaporator efficiency reaches the highest value with R113 (85.81%), while R227ea (75.5%) is the lowest value. Pump efficiency remains constant at similar levels (around 75%). For turbines, all fluids have similar isentropic efficiency values (85%). R123 fluid provides the highest net power with 261.3 kW, while R227ea provides the lowest power with 217.46 kW. Flow rates show the highest values for R113 (13.11 kg/s) and the lowest values for R600 (4.143 kg/s).

The integration of coal gasification and waste heat recovery in advanced technologies holds significant promise for cleaner and more efficient energy production. Utilizing such integrated systems can lead to the generation of combustible gases with high thermal value while mitigating environmental impacts. It is anticipated that this study will contribute to future research endeavors focused on leveraging various renewable energy sources and enhancing sustainability practices.

DECLARATION OF ETHICAL STANDARDS

The author declares to comply with all ethical guidelines, including authorship, citation, data reporting, and original research publication.

CREDIT AUTHORSHIP CONTRIBUTION STATEMENT

All authors made equal contributions to this study

DECLARATION OF COMPETING INTEREST

The author declares that he has no known competing financial interests or personal relationships that could have appeared to influence the work reported in this paper.

FUNDING / ACKNOWLEDGEMENTS

The author declares that he has not received any funding or research grants during the review, research, or assembly of the article

DATA AVAILABILITY

Data will be made available on request.

5. REFERENCES

[1] Türkiye Kömür İşletmeleri Kurumu, "Temiz Kömür Teknolojileri", Erişim Tarihi: [07.07.2019], https://www.tki.gov.tr/temiz-komur-teknolojileri

[2] E. Hacıoğlu and M. Ece, "Kömürün Gazlaştırılması", Erişim Tarihi: [07.07.2019], https://www.geocities.ws/naci_kucukkaya/komur.htm

[3] L. Pierobon, M. Rokni, U. Larsen and F. Haglind, "Thermodynamic analysis of an integrated gasification solid oxide fuel cell plant combined with an organic Rankine cycle." Renewable Energy, 60, 226-234. 2013.

[4] O. J. Ogorure, F. Heberle and D. Brüggemann, "Thermodynamic analysis of a combined Organic Rankine Cycle (ORC) with Proton Exchange Membrane Electrolyzer (PEME) in an integrated biomass conversion system." *In Proceedings of the 6th International Seminar on ORC Power Systems*. 2021.

[5] J. Chen, W. Xu, F. Zhang, H. Zuo, E. Jiaqiang, K. Wei and Y. Fan, "Thermodynamic and environmental analysis of integrated supercritical water gasification of coal for power and hydrogen production." *Energy Conversion and Management*, 198, 111927. 2019.

[6] S. S. Seyitoglu, I. Dincer and A. J. I. J. O. H. E. Kilicarslan, "Energy and exergy analyses of hydrogen production by coal gasification." *International Journal of Hydrogen Energy*, 42(4), 2592-2600. 2017.

[7] L. E. Méndez-Cruz, M. Á. Gutiérrez-Limón, H. Lugo-Méndez, R. Lugo-Leyte, T. Lopez-Arenas and M. Sales-Cruz, "Comparative Thermodynamic Analysis of the Performance of an Organic Rankine Cycle Using Different Working Fluids." *Energies*, 15(7), 2588. 2022.

[8] Kılıç, B., & Arabacı, E. (2019). Alternative approach in performance analysis of organic rankine cycle (ORC). Environmental Progress & Sustainable Energy, 38(1), 254-259.

[9] Khatoon, S., Almefreji, N. M. A., & Kim, M. H. (2021). Thermodynamic study of a combined power and refrigeration system for low-grade heat energy source. Energies, 14(2), 410.

[10] Chowdhury, J. I., Asfand, F., Hu, Y., Balta-Ozkan, N., Varga, L., & Patchigolla, K. (2019, January). Waste heat recovery potential from industrial bakery ovens using thermodynamic power cycles. In ECOS 2019-Proceedings of the 32nd International Conference on Efficiency, Cost, Optimization, Simulation and Environmental Impact of Energy Systems (pp. 2435-2441). Institute of Thermal Technology.

[11] Jeong, J., & Kang, Y. T. (2004). Analysis of a refrigeration cycle driven by refrigerant steam turbine. International journal of refrigeration, 27(1), 33-41.

[12] Sun, X., Liu, L., Zhang, T., & Dai, Y. (2024). Multi-objective optimization of a Rectisol process integrated with compression-absorption cascade refrigeration system and ORC for waste heat recovery. Applied Thermal Engineering, 244, 122611.

[13] Rad, H. N., Ghasemi, A., & Marefati, M. (2024). Cost and environmental analysis and optimization of a new and green three-level waste heat recovery-based cogeneration cycle: A comparative study. Heliyon, 10(7).

[14] Tera, I., Zhang, S., & Liu, G. (2024). A conceptual hydrogen, heat and power polygeneration system based on biomass gasification, SOFC and waste heat recovery units: Energy, exergy, economic and emergy (4E) assessment. Energy, 295, 131015.

[15] Braimakis, K. (2024). Mapping the waste heat recovery potential of CO_2 intercooling compression via ORC. International Journal of Refrigeration, 159, 309-332.

[16] Choudhary, N. K., Deep, A. P., & Karmakar, S. (2024). Thermodynamic Analysis of Integrated Gasification Combined Cycle Integrated with Organic Rankine Cycle for Waste Heat Utilization. Waste and Biomass Valorization, 1-19.

[17] Aryanfar, Y., Mohtaram, S., Alcaraz, J. L. G., & Sun, H. (2023). Energy and exergy assessment and a competitive study of a two-stage ORC for recovering SFGC waste heat and LNG cold energy. Energy, 264, 126191.

[18] Li, L., Qian, J., Teng, S., Zhang, Y., Yin, J., & Zhou, Q. (2023). Comparative analysis and optimization of waste-heat recovery systems with large-temperature-gradient heat transfer. Applied Thermal Engineering, 234, 121179.

[19] Yan, L., Liu, J., Ying, G., & Zhang, N. (2023). Simulation analysis of flue gas waste heat utilization retrofit based on ORC system. Energy Eng, 120, 1919-38.

[20] Ja'fari, M., Khan, M. I., Al-Ghamdi, S. G., Jaworski, A. J., & Asfand, F. (2023). Waste heat recovery in iron and steel industry using organic Rankine cycles. Chemical Engineering Journal, 146925.

[21] Mahmoud, M., Naher, S., Ramadan, M., Abdelkareem, M. A., Jaber, H., & Olabi, A. G. (2023). Investigation of a ground-cooled organic Rankine cycle for waste heat recovery. International Journal of Thermofluids, 18, 100348.

[22] Cui, F., An, D., Teng, S., Lin, X., Li, D., & Xi, H. (2023). Cogeneration systems of solar energy integrated with compressed air energy storage systems: A comparative study of various energy recovery strategies. Case Studies in Thermal Engineering, 51, 103521.

[23] Y. A. Cengel and Boles M.A. Boles, "Thermodynamics: an engineering approach." *McGraw-Hill New York*; 2011.

[24] I, Dincer and M. A. Rosen, "Exergy: energy, environment and sustainable development." *Elsevier Science*; 2012.

[25] A. Steinfeld and P. V. Zedtwitz, "The Solar Thermal Gasification of Coal- Energy Conversion Efficiency and CO_2 Mitigation Potential".*Energy*, Switzerland. 2003.

[26] Z. K. Telli, "Yakıtlar ve Yanma", *Akdeniz Üniversitesi Isparta Mühendislik Fakültesi Yayınları,* Yayın No:17, Isparta. 1984.

[27] P. V. Zedtwitz and A. Steinfeld, "The Solar Thermal Gasification of Coal- Energy Conversion Efficiency and CO_2 Mitigation Potential". *Energy*, Switzerland. 2003

[28] Klein SA. Engineering Equation Solver(EES), F-Chart Software, Version 10.835-3D. 2020

[29] İ. Üçgül and T. Koyun, "Theoretical Investigation of Solar Gasification of Different Types of Lignite Coal." *Yekarum*, 4(1), 7-15. 2019.

[30] M. Shoaei, A. Hajinezhad, and S. F. Moosavian, "Design, energy, exergy, economy, and environment (4E) analysis, and multi-objective optimization of a novel integrated energy system based on solar and geothermal resources," *Energy*, vol. 280, p. 128162, 2023.